Journal of Zoology | ZSL LIVING CONSERVATION

Feeding habits of extant and fossil canids as determined by their skull geometry

Journal:	*Journal of Zoology*
Manuscript ID:	JZO-09-14-OM-281.R1
Manuscript Type:	Original Manuscript
Date Submitted by the Author:	n/a
Complete List of Authors:	Meloro, Carlo; Liverpool John Moores University, Research Centre in Evolutionary Anthropology and Palaeoecology, School of Natural Sciences and Psychology Hudson, Angela; Liverpool John Moores University, Research Centre in Evolutionary Anthropology and Palaeoecology, School of Natural Sciences and Psychology Rook, Lorenzo; Università di Firenze, Dipartimento di Scienze della Terra
Keywords:	Canidae, geometric morphometrics, skull shape, diet, hypercarnivore

Feeding habits of extant and fossil canids as determined by their skull geometry

Carlo Meloro[1], Angela Hudson[1], Lorenzo Rook[2]

[1] Research Centre in Evolutionary Anthropology and Palaeoecology, School of Natural Sciences and Psychology, Liverpool John Moores University, James Parsons Building, Byrom Street, Liverpool L3 3AF, United Kingdom

[2] Dipartimento di Scienze della Terra, Università di Firenze, via G. La Pira, I-50121 Firenze (Italy)

Correspondence

Carlo Meloro, Research Centre in Evolutionary Anthropology and Palaeoecology, School of Natural Sciences and Psychology, Liverpool John Moores University, James Parsons Building, Byrom Street, Liverpool L3 3AF, United Kingdom

e-mail: C.Meloro@ljmu.ac.uk

Short title: Canidae skull shape

Abstract

The canids belong to one of the most prominent families of mammalian carnivores. Feeding adaptations of extant species is well documented by field observations; however we are still missing palaeoecological insights for many enigmatic fossil specimens. We employ geometric morphometrics to quantify skull size and shape in extant and fossil members of the Canini tribe, inclusive of jackals and wolf-like taxa. Skull data are tested to identify correlates of dietary adaptations in extant species for predicting adaptations in fossils. Main vectors of shape variation correlate with the relative skull-palatal length, the position of the upper carnassial tooth and the anterior tip of the secondary palate. Allometry occurs in the palatal shape but size explains only a small fraction (about 4%) of shape variance.

Although we quantified only palatal and tooth shape for the inclusion of fragmentary fossils, discriminant function analysis successfully classify extant Canini in dietary groups (small, medium and large prey specialist) with 89% of accuracy. The discriminant functions provide insights into many enigmatic specimens such as *Eucyon adoxus* (= small prey), fossil jackal-like from Koobi Fora formation (= small prey) and the Plio-Pleistocene Old World canid guild (*Canis etruscus*, *C. arnensis* and *Lycaon falconeri*). Clearly both skull size and shape are excellent predictors of feeding habits in Canini thus also provide information about fossil taxonomic affinities.

Keywords: *Canidae*, *geometric morphometrics*, *skull shape*, *diet, hypercarnivore*

Introduction

Members of the family Canidae have successfully invaded every continent, except Antarctica, occupying a multitude of ecological niches, which is a testament to their adaptability in the present and in the past (Sillero-Zubiri *et al.*, 2004). The most updated molecular phylogeny (Lindbald-Toh *et al.*, 2005) identified distinct clades within the Canidae: i) the redfox-like clade, the South American clade, the wolf-like clade and the grey and island fox clade. This study will focus on the wolf-like clade (tribe Canini), which exhibit one of the most complete fossil record in the Old World (Tedford *et al.*, 1995, 2009). Tedford *et al.* (2009) recently provided a morphological phylogeny merging both extant and fossil species although functional morphology of many enigmatic fossil specimens is still obscure and difficult to characterise (e.g. the genus *Eucyon*, or the wolf-like *Canis etruscus*; Cherin *et al.*, 2014).

The wolf-like clade had an explosion of forms during the Plio-Pleistocene so that biochronology considers such a proliferation of species in the Old World into a separate faunal event (the wolf event, c.ca 2.0 Ma; Azzaroli, 1983; Azzaroli *et al.*, 1988; Torre *et al.*, 1992, 2001; Rook & Torre, 1996a; Sardella & Palombo, 2007; Rook & Martínez-Navarro, 2010; Sotnikova & Rook, 2010). Palaeoecology of many of these canids represented by a coyote-like (*Canis arnensis*), a small wolf-like (*Canis etruscus*) and an African hunting dog-like (*Lycaon falconeri* group; Rook, 1994; Martinez-Navarro & Rook, 2003) was pioneered by Kurtén (1974) and Palmqvist *et al.* (1999) and later reconsidered by Meloro (2011) in a study on mandible shape. Here we aim to investigate skull shape that is expected to provide better insights into feeding ecology of extant, hence fossil Canini.

There have been numerous studies on the relationship between diet and craniodental form in Carnivora and canids in particular (Biknevicius & Ruff, 1992; Van Valkenburgh *et*

al., 2003; Sacco & Van Valkenburgh, 2004; Christiansen & Adolfssen, 2005; Christiansen & Wroe, 2007). Within canids, a shorter snout indicates larger moment arms for the temporalis and masseter muscles (Damasceno *et al*., 2013) and the canines are closer to the fulcrum, both creating a more powerful bite force (Christiansen & Adolfssen, 2005; Christiansen & Wroe, 2007). This is interpreted as an adaptation to kill large prey and can be detected in living and extinct canid tribes (Valkenburgh & Koepfli, 1993; Andersson, 2005; Van Valkenburgh *et al*., 2003; Slater *et al*., 2009).

Early morphometric attempts on Canidae general morphology already elucidated cophenetic similarities in relation to their taxonomy and ecology (Clutton-Brock *et al.*, 1976). By focusing on palatal and upper teeth morphology with geometric morphometric techniques we intend to capture both size and shape aspects relevant to interpret fossil species. Geometric morphometrics has the advantage of allowing clear data visualisation in multivariate shape space (Adams *et al.*, 2004, 2013; Lawing & Polly, 2009). In addition, shape distances can be employed to infer morphological similarities: this is a straightforward way to compare data between living and fossil specimens (Caumul & Polly, 2005; Meloro *et al*., 2008; Meloro, 2011). Due to the tendency in canids of increasing body mass towards their evolution in relation to ecological feeding specialisation (Van Valkenburgh *et al.*, 2004) we will also explore skull size as possible proxy for predicting diet in extant and fossil species.

Materials and Methods

Sample Size

Skulls belonging to 102 specimens (85 extant and 17 fossils) were included in this study (Appendix 1). Our sample is representative of the broad diversity within the *Canis* clade including jackals and wolf-like ecomorphs (9 extant and 10 fossil species, Table 1). All extant specimens belong to wild captured individuals. Both male and female skulls were used indistinctively because sexual dimorphism is considered a negligible source of variance to infer dietary adaptations from the skulls. Indeed, sexual dimorphism within canids is generally small (Van Valkenburgh & Gittleman, 1997) and the gender is unknown for many fossil specimens.

For fossil species we used the nomenclature finalised by Tedford *et al.* (2009). The small genera *Eucyon* and *Cynotherium* (with the species *Eucyon adoxus* and *Cynotherium sardous*) were also considered for their unequivocal affinities with extant *Canis*-like species (Rook, 2009; Lyras *et al.*, 2006).

Data Capture

Digital photographs were collected on skulls positioned in ventral view by Meloro C. using a Nikon 995 at a 1 metre distance. A spirit level was positioned on the palate of the skull to ensure parallelism between camera optical plan and the flattest region of the skull. On each skull, 15 landmarks were recorded by one of us (Hudson A.) in the palate region to capture details of tooth and cusp positioning using the software tpsDig2 ver. 2.17 (Rohlf, 2013a) (Fig. 1). Landmarks 1-2 record the width of the incisor arch, 3-4 the relative size of canine, landmark 5 is at the anterior tip of P3, 6 to 10 relative size of the upper carnassial (P4) together with the positioning of the main cusps, 10-14 covers the M1 morphology and landmark 15 is the most posterior point delimiting the end of the palate.

Cusp positions were recorded on P4 and M1 as good proxy for dietary adaptations but also to understand possible phylogenetic affinities between extant and fossil taxa (cf. Rook & Torre, 1996; Brugal & Boudadi-Maligne, 2010). The posterior part of the skull and the zygomatic arch were not covered by landmarks because they were not present in many of the analysed fossils.

Intra-individual error in landmarking was assessed using three landmarked replicas for three specimens. There were no differences in the variance of coordinates values between replicas (ANOVA and MANOVA $p > 0.9$).

Geometric Morphometrics

Landmark coordinates were aligned using Generalised Procustes superimposition (Rohlf & Slice, 1990) with the software tpsRelw ver. 1.53 (Rohlf, 2013b). The software performed three operations: translation, rotation and scaling to transform the original 2D coordinates of landmarks into shape coordinates. A Principal Component analysis of the covariance matrix of the shape coordinates was then computed. Shape variation along each principal component axis was visualised using a thin-plate spline (Bookstein, 1991). Thin plate splines visualize shape variation assuming that the average consensus configuration has no deformation and line on an infinite metal plane whose bending describe shape changes (Zelditch *et al.*, 2004).

The size of landmark configuration was extrapolated from the raw coordinates via centroid size (=the square root of the mean squared distance from each landmark to centroid of the landmark configuration Bookstein, 1989). In order to scale centroid size to the mean, natural log transformation was used (cf. Meloro *et al.*, 2008).

Feeding Categories

For each extant species, a feeding category was assigned following multiple references. Van Valkenburgh (1989) grouped extant carnivores into three dietary categories: hypercarnivores, mesocarnivores and hypocarnivores. However, because there are no hypocarnivores in the sample for this study, Palmqvist *et al.*'s (1999) grouping of canids was also considered. Using both categorisations as a template, diet categories were assigned as small prey (mesocarnivore, mostly feeding on rodents and lagomorphs), medium prey (mesocarnivore that can include a wider range of prey sizes) and large prey (hypercarnivore, mostly preying on large ungulates). Extant jackals and the Ethiopian wolf belong to the category "small prey", while the grey wolf, the African wild dog and the dhole are categorised as "large prey" (cf. Slater *et al.*, 2009). The coyote and the dingo were categorised as "medium prey" because of their broad adaptability in also hunting large prey in group (Gese *et al.*, 1988; Lingle, 2002; Sillero-Zubiri *et al.*, 2004; Christiansen & Wroe 2007; Letnic *et al.*, 2012).

Data Analyses

Differences in skull size and shape due to diet were preliminary tested using ANOVA and parametric and non-parametric MANOVA. Due to the large number of independent shape variables a selection of Principal Components (the one explaining at least 95% of variance) was employed to validate MANOVA models based on the full set of shapes (cf. Meloro & O'Higgins, 2011).

Additionally, allometry was tested in order to identify the possible influence of size on shape data (Mitteroecker *et al.*, 2013). A multivariate regression was employed to identify and visualise allometric signal in the whole sample of 102 skulls using thin plate spline.

Discriminant Function Analysis was employed to provide prediction for fossil species using diet categories as factor and shape coordinates and natural log centroid size as independent variables. To considerably reduce the number of independent dietary predictors a stepwise procedure was applied: a variable was entered into the model if the probability of its F value was bigger than 0.05 and was removed if the probability was less than 0.10. Meloro (2011) consistently demonstrated the importance of including mandibular size as a predictor of feeding adaptation in Carnivora. We expect this to also hold for skull size in canids.

An UPGMA cluster analysis was employed to identify cophenetic similarities between fossil and extant specimens. Averaged shape coordinates were first computed for each extant and fossil species, then procustes distances calculated to construct the clustering UPGMA tree (cf. Meloro, 2011).

Results

Skull shape

Variability in skull shape is significantly reduced by using Principal Component analysis, with the first 12 PC axes explaining 95.26% of total shape variance. PC1 and PC2 explain 45.76% and 15.60% of total variance respectively and their combination show substantial differences between small jackal-like and large wolf-like species (Fig. 2). At the extreme negative of PC1 *Canis simensis* is represented by a thin and slender palate with relatively short incisor row and canine but long snout, on the opposite of PC1 *Lycaon pictus* together with *Cuon* share a much larger palate with relatively larger upper carnassial and M1. PC2 is highly influenced by position of landmark 15 and separates jackals and hypercarnivore *Lycaon-Cuon* from grey wolf and coyote. Fossil canids are evenly spaced in different areas of

the morphospace and tend generally to occupy less extreme scores with the exception of *Lycaon falconeri* (at the extreme positive PC1 and negative PC2).

MANOVA shows significant differences between diet in skull shape (represented by the first 12 PCs) (Wilk's lambda = 0.164, F = 8.677, df = 24, 142, $p < 0.0001$). Same applies when non-parametric MANOVA is computed after permuting Euclidean distances between dietary groups 9,999 times (F = 16.74, $p < 0.0001$).

Skull shape differs significantly also between dietary categories (Wilk's lambda = 0.050, F = 3.88, df = 52, 58, $p < 0.0001$).

Skull size and allometry

Skull size (here represented by ln centroid size of the landmark configuration) was normally distributed across dietary categories (P values after Kolgomorov-Smirnoff always > 0.06). This allowed us to perform an ANOVA test that shows significant differences between small, medium and large prey consumers (F = 22.963, df = 2, 82, $p < 0.0001$; Fig. 3a). Due to significant differences in homogeneity of variance test (Levene statistic 5.702, df = 2, 82, p = 0.005), Dunnett's T3 was employed. This test shows significant differences in size between all the diet categories ($p < 0.025$ in all pairwise comparisons).

A significant allometric component was also detected even if ln centroid size explains only a very small fraction of total shape variance (Wilks' Lambda = 0.343, F = 5.531, df = 26, 75, $p < 0.0001$; 4.11% of variance). Indeed, deformation grids depicted only a small deformation occurring mostly in the canine and upper carnassial (P4) areas (Fig. 3b). A closer inspection of allometry shows significant negative correlation only between ln CS and PC3 (10.12% of

variance, r = -0.541), PC8 (1.85% of variance, r = -0.281) and PC10 (1.20 % of variance, Spearman r = -0.119).

Dietary discrimination

After stepwise only five out of 30 shape coordinates and ln Centroid Size were selected by the Discriminant Function analysis. Two significant DF were extracted to differentiate dietary groups (DF1: 93.8% variance, Wilk's lambda = 0.113, χ^2 = 173.66, df = 12, p < 0.0001; DF2: 6.2% variance, Wilk's lambda = 0.733, χ^2 = 24.691, df = 5, p < 0.0001).

Percentage of correctly classified cases after cross-validation is high (Small = 86.5%; Medium = 86.7% and Large = 93.9%).

DF1 was positively and significantly loaded on ln CS (r = 0.314), procustes coordinate X of the landmark 6 (the anterior tip of P4, r = 0.251), and negatively on coordinate Y for landmark 1 (tip of the snout, r = -0.586). DF2 correlated positively with coordinate Y of landmark 3 (anterior tip of the canine, r = 0.841) and negatively on coordinate X of landmark 11 (M1 paracone, r = 0.478), Y for landmark 13 (anterior tip of M1, r = 0.398).

The deformation grids were obtained after regressing discriminant function scores vs shape coordinates. They show how species adapted to kill large prey at the positive DF1 are characterised by a shorter and thicker muzzle opposite to species adapted in killing small prey (Fig. 4). Medium prey specialists exhibit intermediate DF1 scores and negative DF2 scores. They are discriminated by "small prey" due to a thin and long muzzle with relatively bigger carnassial (P4) and M1 (Fig. 4).

Fossil specimens are predicted to cover the whole range of dietary adaptations of extant Canini (Table 2). Species represented by multiple specimens are sometimes predicted into

more than one category with the exception of the dire wolf for which both specimens are consistently categorised as predators of large prey. *Eucyon adoxus*, *Cynotherium sardous*, *C.* cf. *mesomelas* and one specimen of *C. arnensis* and *C. etruscus* follow within the "small prey" category, while *C. lupus* from Romanelli, one specimen of *C. arnensis* and one of *C. chihliensis* follow within category "medium prey". All large fossil hypercarnivores are classified as "Large" (Table 2).

Clustering

The UPGMA based on procustes distances yields a cophenetic cluster with a high cophenetic correlation (r = 0.882). There is a mix of ecological and taxonomic signal with some fossil taxa clustering together due to their unique affinities (e.g., *E. adoxus* with *C.* cf. *mesomelas* from Olduvai Gorge). The fossil hunting dog *L. falconeri* is clearly an outgroup that allows identifying three main groups: 1. a cluster showing the affinity of the extant Ethiopian wolf (*C. simensis*) with the prehistoric *C. arnensis*; 2. a cluster that separates extant jackal-like forms (inclusive of the fossil hypercarnivore *C. antonii* and wolf-like *C. etruscus* and *C. mosbachensis*) from grey wolf cluster inclusive of the dingo and the dire wolf; 3. hypercarnivore cluster inclusive of fossil *C. africanus*, extant *Lycaon* and *Cuon* and a fossil grey wolf from Spain.

Discussion

With no doubt, skull size and shape of extant Canini can strongly be linked to their feeding habits (Van Valkenburgh & Koepfli, 1993; Van Valkenburgh *et al.*, 2003; Andersson, 2005; Slater *et al.*, 2009; Damasceno *et al.*, 2013). By investigating only the palate, we critically

limited the amount of size and shape information, but demonstrate that this area is ecologically and taxonomically informative. Indeed, MANOVA and ANOVA show significant differences between feeding categories re-defined to fit the broad dietary variation observed in the Canini tribe (Sillero-Zubiri *et al.*, 2004).

The palate of species adapted to hunt small prey is thin, longer and characterised by relatively shorter P4 and M1. All these adaptations can be observed in extant jackals and especially in the Ethiopian wolf (*C. simensis*) that occupy the extreme morphological variation on the first RW (Fig. 2). This confirms early morphometric observation by Rook & Azzaroli Puccetti (1996) and functional morphology by Slater *et al.* (2009). In contrast, the grey wolf, African hunting dog and the dhole cluster together in the morphospace (Fig. 2) for their typical hypercarnivorous traits (Van Valkenburgh, 1991): a short and broad muzzle with larger incisors and canine (cf. Andersson, 2005) and relatively larger upper carnassial. All these features correlate with higher bite forces (Christiansen & Wroe, 2007; Damasceno *et al.*, 2013) hence the ability to kill prey much larger than themselves. Not surprisingly, these morphologies are well separated from the other feeding groups, supporting the highest classification rate in the Discriminant Function analysis.

In agreement with previous findings on the mandible, it is not only palatal shape that is a good discriminator of diet in extant Canini but also its size (cf. Meloro, 2011). The ecological continuum observed in Canini diet is reflected into skull morphology so that intermediate sized dogs (the coyote and the dingo) show intermediate skull shapes allowing them to expand feeding niches under different circumstances. Indeed, the medium size canid hunters possess relatively larger upper carnassial and M1 but retain a longer and thin snout (in the case of the coyote) or have a broad palate but not so extreme as in *Cuon* or *Lycaon* (the dingo in Fig. 2).

It is important to note that although an allometric component was detected in our data, it accounts only for a small percentage of shape variance. When size generally explains large portion of shape variance it is common practice to use "size-free" shape residuals, although this correction generally does not provide additional insights (cf. Meloro *et al.*, 2014). Mitteroecker *et al.* (2013) recently argued the necessity to take size into account by actually adding, and not removing this variable from subsequent analyses. Our results confirm such assertion thus supporting the combined interpretation of palatal size and shape to infer palaeoecology of fossil species.

Fossil genera *Eucyon* and *Cynotherium* cluster well within the morphological variation of extant Canini confirming previous taxonomic observations on their affinities (Rook, 2009; Lyras *et al.*, 2010). The Principal Component plot shows similar scores between these taxa and the extant jackals, both clustering within the range of the side-striped jackal (Fig. 2). Consequently, the dietary reconstruction as specialist hunter of small prey fits well with previous attempts for the *Cynotherium* (cf. Abbazzi *et al.*, 2005; Lyras *et al.*, 2006) and underlines the strong affinity of *Eucyon* (at least for the species *E. adoxus*) with jackals.

Dietary reconstruction for Plio-Pleistocene dogs confirms the puzzling evolution of the Etruscan wolf (*Canis etruscus*) and the coyote-like *Canis arnensis* while supporting the hypercarnivorous traits of *Lycaon falconeri*, *C. antonii* and *C. africanus* (cf. Rook, 1994; Tedford *et al.*, 2009). Both *C. etruscus* and *C. arnensis* specimens occupy more than one dietary classification in agreement with previous studies (Cherin *et al.*, 2014; Flower & Shreve, 2014; Meloro, 2011). However, there is a clear size partitioning with the Arno dog being classified as small-medium, while only one *C. etruscus* is predicted as small prey with the others grouped into large prey category. Due to ecological character displacement, it is possible that morphological variation in these taxa was broad and influenced by presence or absence of larger competitors (García & Virgós, 2007).

Diet of the large American dire wolf fits consistently with previous palaeoecological reconstructions (Anyonge & Baker 2006; Meloro, 2011, 2012), while new insights emerge for *Canis chihliensis* from the lower Pleistocene of China. Tong *et al.* (2012) identified a mosaic of features combining hypercarnivorous dentition with a relatively small size compared to the grey wolf. Consequently, the size constraint on hunting behaviour supports our prediction of *C. chihliensis* as an adaptable hunter within the medium category (cf. dingo, see also Fig. 2). For the middle Pleistocene *C. mosbachensis* a large size categorisation also seems likely based on its morphofunctional similarity to the grey wolf (cf. Flower & Shreve, 2014). Diet prediction for the wolf of Romanelli cave also fits within the category "Medium". Although Sardella *et al.* (2014) confirmed its taxonomic affinity to the grey wolf, they also pointed out how its smaller size confounded previous taxonomic attempts of this species into golden jackal or *C. mosbachensis*. The grey wolf is highly flexible in size and ecology (Sillero-Zubiri *et al.*, 2004). Such flexibility has been observed in prehistoric specimens (Flower & Shreve, 2014) as well as ancestral forms supporting possible ecogeographical differentiation in the past. Comfortably the fossil grey wolf from Spain is predicted as large prey specialist.

The enigmatic *Canis* cf. *mesomelas* from Koobi Fora deserves a separate note. Werdelin & Lewis (2005) and Werdelin & Peigné (2010) reviewed the rich Plio-Pleistocene East African carnivore fauna. Taxonomy of jackals is not clear yet and there seems to be evidence for different ecomorphotypes in hominin fossil sites. Our analysis suggests the Koobi Fora specimen being adapted for hunting small-sized prey. Interestingly, the UPGMA analysis (Fig. 5) supports shape similarity not with extant jackals, but with the Mio-Pliocene genus *Eucyon* suggesting that it was a distinct (but ecologically equivalent to the extant jackal) morphotype.

For the other taxa, the UPGMA cluster analysis shows a mixed signal based on shape data. P4 and M1 morphology are phylogenetic characters in Canini (Tedford *et al.*, 2009) although the presented UPGMA (Fig. 5) cannot disentangle the ecological from the phylogenetic signal (cf. Meloro, 2011). The clustering of *C. africanus* within *Lycaon-Cuon* confirms the grouping proposed by Rook (1994). However, the palate of *Lycaon falconeri* from Valdarno and that of *C. antonii* are highly distinct from *C. africanus*. Ecogeographical and temporal variation could explain such a pattern even if larger and more complete sample is needed to prove this assertion. The grouping of *E. adoxus* with the jackal from Koobi Fora suggests how distinct the morphology is from these Plio-Pleistocene forms with no extant relatives, even if their smaller size supports ecological similarities with jackals and coyotes. *Cynotherium* is also enigmatically positioned (although outside of the wolf cluster) while the cluster of *C. etruscus* with *C. adustus* also does not support the wolf phylogenetic hypothesis (cf. Tedford *et al.*, 2009). Interestingly, recent research on African jackals supports the identification of a wolf North African subspecies (*Canis lupus lupaster*) that was morphologically ascribed to the golden jackal (Gaubert *et al.*, 2013) suggesting how puzzling morphological characters can be not only in fossil but also in extant species. The Romanelli grey wolf is an outgroup within the wolf cluster while the dire wolf is grouped with the dingo and grey wolf. Extant *Lycaon* and *Cuon* clusters together consistently with their hypercarnivorous feeding habits.

Members of Canini clearly occupied a broad range of ecological niches since the Pliocene then differentiating during Early Pleistocene with the evolution of modern taxa (Sotnikova & Rook, 2010). Such a rapid differentiation resulted in a high flexibility of ecomorphological skull traits whose combination provide robust palaeoecological insights.

Acknowledgments

We are grateful to the curators of different museum institutions for kindly providing access to osteological collections: P. Jenkins, L. Tomsett, R. Portela-Miguez, A. Salvador, D. Hills, J. J. Hooker, P. Brewer, and A. Currant (British Museum of Natural History, London); E. Cioppi (Museo di Storia Naturale Università di Firenze, Florence); M. Reilly and J. Liston (Huntherian Museum and Art Gallery, University of Glasgow, Glasgow); B. Sanchez, J. Morales, J. Cabarga, and J. B. Rodríguez (Museo Nacional de Ciencias Naturales, Madrid); A. Kitchener (Royal Museum of Scotland, Edinburgh); E. Gilissen and W. Wendelen (Royal Museum for Central Africa, Tervuren); E. Mbua, M. Mungu, F. Nderitu and O. Mwebi (Kenya National Museum, Nairobi). Visit to the Museo Nacional de Ciencias Naturales and Royal Museum of Central Africa were supported by the Synthesys grants ‘‘Feeding habits in extinct European carnivores” (ES-TAF 858) and “Ecomorphology of extant African carnivores’’ (BE-TAF 4901) to C. Meloro while part of the comparative analyses were supported by Synthesys grants “Craniodental morphometric analysis of living and fossil jackals” FR-TAF 3311 and BE-TAF 3607 to L. Rook. Access to the collections of National Museum of Kenya was kindly granted by the Governments of Kenya and Tanzania and the Leverhulme Trust project ‘‘Taxon-Free Palaeontological Methods for Reconstructing Environmental Change’’ (F/00 754/C). Finally we would like to thank two anonymous reviewers and the journal editor for their insights and care that considerably improved the quality of our manuscript.

References

Abbazzi, L., Arca, M., Tuveri, C., Rook L. & (2005). The endemic canid *Cynotherium* (Mammalia, Carnivora) from the Pleistocene deposits of Monte Tuttavista (Nuoro, Eastern Sardinia). *Riv. Ital. Paleontol. S.* **111**, 493–507.

Adams, D. C., Rohlf, F. J., & Slice, D. E. (2004). Geometric morphometrics: Ten years of progress following the 'revolution'. *Ital. J. Zool.* **71**, 5–16.

Adams, D. C., Rohlf, F. J., & Slice, D. E. (2013). A field comes of age: geometric morphometrics in the 21st century. *Hystryx, the Italian Journal of Mammalogy* **24**, 7–14.

Andersson, K. (2005). Were there pack-hunting canids in the Tertiary, and how can we know? *Paleobiology* **31**, 56–72.

Anyonge, W., & Baker, A. (2006). Craniofacial morphology and feeding behavior in Canis dirus, the extinct Pleistocene dire wolf. *J. Zool.* **269**, 309–316.

Azzaroli, A. (1983). Quaternary Mammals and the End-Villafranchian Dispersal event - a turning point in the history of Eurasia. *Palaeogeogr., Palaeoclimatol., Palaeoecol.* **44**, 117–139.

Azzaroli, A., De Giuli, C., Ficcarelli, G., & Torre, D. (1988). Late Pliocene to early mid-Pleistocene mammals in Eurasia: faunal succession and dispersal events. *Palaeogeogr., Palaeoclimatol., Palaeoecol.* **66**, 77–100.

Biknevicius, A. R. and Ruff, C. B. 1992. The structure of the mandibular corpus and its relationship to feeding behaviors in extant carnivorans. *J. Zool.* **228**, 479–507.

Bookstein, F. L. 1989. 'Size and Shape': a comment on semantics. *Syst. Zool.* **38**,173–180.

Bookstein, F. L. 1991. Morphometric tools for landmark data. Geometry and Biology. Cambridge University Press, New York.

Brugal, J.P., & Boudadi-Maligne, M. (2010). Quaternary small to large canids in Europe: taxonomic status and biochronological contribution. *Quat. Int.* **243**, 171–182

Caumul, R., & Polly, P.D. (2005). Phylogenetic and environmental components of morphological variation: skull, mandible and molar shape in marmots (Marmota, Rodentia). *Evolution* **59**, 2460–2472.

Cherin, M., Bertè, D.F., Rook, L., & Sardella, R. (2014). Re-defining *Canis etruscus* (Canidae, Mammalia): a new look into the evolutionary history of Early Pleistocene dogs supported by the outstanding fossil record from Pantalla (Perugia, central Italy). *J. Mamm. Evol.* **21**, 95–110.

Christiansen, P., & Adolfssen, J.S. (2005). Bite forces, canine strength and skull allometry in carnivores (Mammalia, Carnivora). *J. Zool.* **266**, 133–151.

Christiansen, P., &Wroe, S. (2007). Bite forces and evolutionary adaptations to feeding ecology in carnivores. *Ecology* **88**, 347–358.

Clutton-Brock, J., Corbet, G.B., & Hills, M. (1976). A review of the family Canidae, with a classification by numerical methods. *Bulletin of the British Museum (Natural History), Zoology* **29**,119–199.

Damasceno, E. M. Hignst-Zaher, E., & Astúa, D. (2013). Bite force and encephalization in the Canidae (Mammalia: Carnivora). *J. Zool.* **290**, 246–254.

Flower, L.O.H., & Shcreve, D.C. (2014). An investigation of palaeodietary variability in European Pleistocene canids. *Quat. Sci. Rev.* in press.

García, N., & Virgós, E. (2007). Evolution of community composition in several carnivore paleoguilds from the European Pleistocene: the role of interspecific competition. *Lethaia* **40**, 33–44.

Gaubert, P., Bloch, C., Benyacoub, S., Abdelhamid, A., Pagani, P. et al. (2012). Reviving the African wolf *Canis lupus lupaster* in North and West Africa: a mitochondrial lineage ranging more than 6,000 km wide. *PLoS ONE* **7(8),** e42740.

Gese, E.M., Rongstad O.J., & Mytton W.R. (1988). Relationship between coyote group size and diet in Southeastern Colorado. *J. Wildl. Manage.* **52**, 647–653.

Gittleman, J. L., & Van Valkenburgh, B. (1997). Sexual size dimorphism in the canines and skulls of carnivores: effects of size, phylogeny, and behavioural ecology. *J. Zool., Lond.* **242**, 97–117.

Kurtén, B. (1974). A history of coyote-like dogs (Canidae, Mammalia). *Acta Zool. Fenn.* **140**, 1-38.

Letnic, M., Ritchie, E.C., & Dickman, C.R. (2012). Top predators as biodiversity regulators: the dingo *Canis lupus dingo* as a case study. *Biol. Rev.* **87**, 390–413.

Lindbald-Toh K., et al. (2005). Genome sequence, comparative analysis and haplotype structure of the domestic dog. *Nature* **438**, 803–819.

Lingle, S. (2002). Coyote predation and habitat segregation of white-tailed deer and mule deer. *Ecology* **83**, 2037–2048.

Lawing, A. M., & Polly, P.D. (2009). Geometric morphometrics: recent applications to the study of evolution and development. *J. Zool.* **280**, 1–7.

Lyras, G.A., van der Geer, A.A.E., Dermitzakis, M., & De Vos, J. (2006). *Cynotherium sardous*, an insular canid (Mammalia: Carnivora) from the Pleistocene of Sardinia (Italy), and its origin. *J. Vert. Paleontol.* **26**, 735–745.

Lyras, G., van Der Geer, A.A.E., Rook, L. 2010. Body size of insular carnivores: evidence from the fossil record. *J. Biogeogr.* **37**, 1007–1021.

Martínez-Navarro, B., & Rook, L. (2003). Gradual evolution in the African hunting dog lineage systematic implications. *C.R. Palevol* **2**, 695–702.

Meloro, C. (2011). Feeding habits of Plio-Pleistocene large carnivores as revealed by the mandibular geometry. *J. Vert. Paleontol.* **31**, 428–446.

Meloro, C. (2012). Mandibular shape correlates of tooth fracture in extant Carnivora: implications to inferring feeding behaviour of Pleistocene predators. *Biol. J. Linn. Soc.*, **106**, 70–80.

Meloro, C., Raia, P., Piras, P., Barbera, C., & O'Higgins. P. (2008). The shape of the mandibular corpus in large fissiped carnivores: allometry, function and phylogeny. *Zool. J. Linn. Soc.* **154**, 832–845.

Meloro, C., & O'Higgins, P. (2011). Ecological Adaptations of mandibular form in fissiped carnivore. *J. Mammal. Evol.* **18**, 185–200.

Meloro, C., Cáceres, N., Carotenuto, F., Sponchiado J, Melo GL. Passaro, F. & Raia, P. (2014). In and out the Amazonia: evolutionary ecomorphology in howler and capuchin monkeys. *Evolutionary Biology* **41**, 38–51.

Mitteroecker, P., Gunz, P., Windhager, S., & Schaefer K. (2013).A brief review of shape, form, and allometry in geometric morphometrics, with applications to human facial morphology. *Hystrix - Italian Journal of Mammalogy* **24**, 59–66.

Palmqvist, P. Arribas, A., & Martinez-Navarro, B. (1999). Ecomorphological study of large canids from the lower Pleistocene of southeastern Spain. *Lethaia*, **32**, 75–88.

Rohlf, F. J. 2013a. tpsDig2 ver.2.16. Ecology & Evolution, SUNY at Stony Brook.

Rohlf, F. J. 2013b. tpsRelw ver.1.53. Ecology & Evolution, SUNY at Stony Brook.

Rohlf, F.J., & Slice, D.E. (1990). Extensions of the Procrustes method for the optimal superimposition of landmarks. *Syst. Zool.* **39**, 40–59.

Rook, L. (1992). "*Canis*" *monticinensis* sp. nov., a new Canidae (Carnivora, Mammalia) from the late Messinian of Italy. *Boll. Soc. Paleontol. I.* **31**, 151–156.

Rook, L. (1994). The Plio-Pleistocene Old World *Canis* (*Xenocyon*) ex. gr. *falconeri*, *Boll. Soc. Paleontol. I.* **33**, 71–82.

Rook, L. (2009). The wide ranging genus *Eucyon* Tedford & Qiu, 1996 (Mammalia, Carnivora, Canidae) in Mio-Pliocene of the Old World. *Geodiversitas* **31**, 723–743.

Rook, L., & Azzaroli Puccetti, M.L. (1996). Remarks on the skull morphology of the endangered Ethiopian jackal, *Canis simensis* Rüppel, 1838. *Memorie Fisiche della Accademia Nazionale dei Lincei*, ser. **9**(7), 277–302.

Rook, L., & Torre, D. (1996). The wolf event in western Europe and the beginning of the Late Villafranchian. *Neues Jahrbuch für Geologie und Paläontologie Monatshefte* 8, 495–501.

Rook, L., & Martínez-Navarro, B. (2010). Villafranchian: The long story of a Plio-Pleistocene European large mammal biochronologic unit. *Quat. Int.* **219**, 134–144.

Rueness, E.K., Asmyhr, M.G., Sillero-Zubiri, C., Macdonald, D.W., Bekele, A., et al. (2011). The cryptic African wolf: *Canis aureus lupaster* is not a golden jackal and is not endemic to Egypt. *PLoS ONE* **6(1)**, e16385.Sacco, T. and Van Valkenburgh, B. 2004. Ecomorphological indicators of feeding behaviour in the bears (Carnivora: Ursidae). *J. Zool.* **263**, 41–54.

Sardella, R., & Palombo, M.R. (2007). The Plio-Pleistocene boundary: which significant for the so-called "wolf-event"? Evidence from Western Europe. *Quaternaire* **18**, 65–71.

Sardella, R., Bertè, D., Lurino, D.A., Cherin, M., & Tagliacozzo, M. (2014). The wolf from Grotta Romanelli (Apulia, Italy) and its implications in the evolutionary history of *Canis lupus* in the Late Pleistocene of Southern Italy. *Quat. Int.* **328-329**, 179–195.

Sillero-Zubiri, C. Hoffmann, M. & Macdonald, D.W. (2004). *Canids: Foxes, Wolves, Jackals and Dogs. Status Survey and Conservation Action Plan*. IUCN/SSC Canid Specialist Group.

Slater, G., Dumont, E. R., & Van Valkenburgh, B. (2009). Implications of predatory specialization for cranial form and function in canids. *J. Zool.* **278**, 181–188.

Sotnikova, M.V., Rook, L. 2010. Dispersal of the Canini (Mammalia, Canidae: Caninae) across Eurasia during the Late Miocene to Early Pleistocene. *Quat. Int.* **212**, 86–97.

Tedford, R. H., Taylor, B. E., & Wang X. (1995). Phylogeny of the Canidae (Carnivora: Canidae): the living taxa. *Am. Mus. Novit.* 3146, 1–37.

Tedford, R. H., Wang, X., & Taylor, B. E. (2009). Phylogenetic systematics of the North American fossil Caninae (Carnivora: Canidae). *B. Am. Mus. Nat. Hist.* **325**, 1–218.

Tong, H., Hu, N., & Wang, X. (2012). New remains of *Canis chihliensis* from Shianshenmiazoui, a lower Pleistocene site in Yanguai, Hebei.*Vertebrat. Palasiatic.* **50**, 335–360.

Torre, D., Ficcarelli, G., Masini, F., Rook, L., & Sala, B. (1992). Mammal dispersal events in the Early Pleistocene of Western Europe. *Courier Forschungs-Institut Senckenberg* **153**, 51–58.

Torre, D., Abbazzi, L., Bertini, A., Fanfani, F., Ficcarelli, G., Masini, F., Mazza, P., & Rook, L. (2001). Structural changes in Italian Late Pliocene - Pleistocene large mammal assemblages. *Boll. Soc. Paleontol. I.* **40**, 303–306.

Van Valkenburgh, B. (1991). Iterative evolution of hypercarnivory in canids (Mammalia: Carnivora): evolutionary interactions among sympatric predators. *Paleobiology* **17**, 340–362.

Van Valkenburgh, B. (1989). Carnivore dental adaptations and diet: a study of trophic diversity within guilds. In *Carnivore Behavior, Ecology, and Evolution, Volume 1*: 410–436. Gittleman, J.L. (Ed.), Cornell University Press, Ithaca, New York.

Van Valkenburgh, B., & Koepfli, K. (1993). Cranial and dental adaptations for predation in canids. *Symposia of the Zoological Society of London* **65**, 15–37.

Van Valkenburgh, B. V. Sacco, T., & Wang, X. (2003). Pack hunting in Miocene borophagine dogs; evidence from craniodental morphology and body size. *B. Am. Mus. Nat. Hist.* **279**, 147–162.

Van Valkenburgh, B., Wang, X., Damuth, J. (2004). Cope's rule, hypercarnivory, and extinction in North American canids. *Science* **306**, 101–104.

Werdelin, L. & Lewis, M.E. (2005). Plio-Pleistocene Carnivora of eastern Africa: species richness and turnover patterns. *Zool. J. Linn. Soc.* 144, 121–144.

Werdelin, L. & Peigné, S. (2010). Carnivora, Chapter: 32. In *Cenozoic mammals of Africa*: 603–657. Werdelin, L., & Sanders, W.J. (Eds.), University of California Press.

Zelditch, M. L. Swiderski, D. L., & Sheets, H. D. (2004). *Geometric Morphometrics for Biologists: A Primer. Second Edition*. Elsevier.

Figures Legend

Figure 1 Skull of *Canis adustus* showing the landmark locations placed on each specimen. (1) tip of the snout defined by middle point between the first two frontal incisors, 2) posterior tip of 3rd incisor, 3) anterior tip of canine, 4) posterior tip of canine, (5) anterior tip of the third premolar, (6, 7, 8, 9, 10) outline of carnassial tooth, (11, 12) cusps of molar, (13) anterior tip of molar, (14) posterior tip of molar, (15) junction of the stiff and hard palate. The distance between 3 and 4 describe canine length. The distance between 8 and 10 describe carnassial tooth length. The distance between 1 and 15 describes snout length. Deviation of the specimens analysed from the consensus configuration of landmarks are shown below the skull. Scale bar equals 1cm.

Figure 2 Plot of the first and second principal components. Thin-plate spline diagrams illustrate patterns of landmark displacements along each warp. Triangles indicate canids in the large dietary category, ellipsoid indicate canids in the medium dietary category and circles indicate canids in the small dietary category. Crosses and stars indicate fossil specimens with an unknown diet category. Below deformation grids from positive to negative RW scores.

Figure 3 (a) Box plot showing differences in natural log transformed centroid size between diet categories of extant specimens of canid skull (the outlier in the "Medium Prey" category is a specimen of *C. latrans*); (b) skull shape deformation related to size from the smallest (*C. mesomelas*) to the largest (*C. dirus*) canid species. Values in parentheses are ln centroid size.

Figure 4 Plot of the first two discriminant functions (DF) extracted from a combination of shape and size variables. Extant specimens are labelled according to their diet categorisation. Fossil specimens are labelled individually. Below deformation grids from positive to negative DF scores.

Figure 5 UPGMA Cluster analysis obtained on procustes distances of averaged sample for 23 canid species.

Tables Legend

Table 1 Skull sample sizes of extant and fossil canid species together with assigned dietary grouping. *Includes subspecies (*Canis lupus gigas* and *Canis lupus pambasileus*); ** includes subspecies (*Cuon alpinus dukhnensis* and *Cuon alpinus javanicus*). Small = mesocarnivore feeding on small prey, medium = mesocarnivore feeding on medium prey, large = hypercarnivore feeding on large prey.

Table 2 Dietary classification provided for fossil specimens using discriminant function analysis. P (D | G) is the probability of membership in a group given the discriminant function score. P (G | D) is the posterior probability based on the sample employed to generate the discriminant functions.

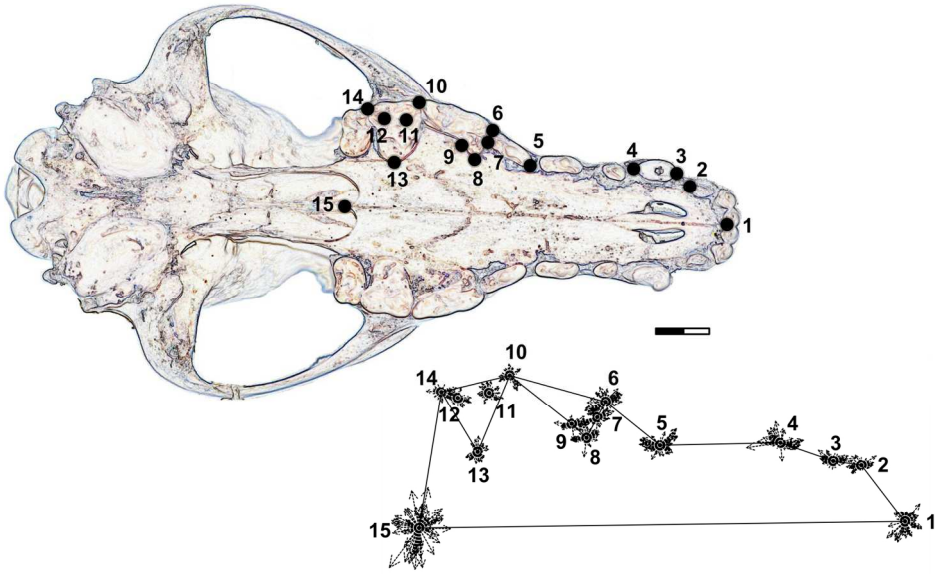

Figure 1 Skull of Canis adustus showing the landmark locations placed on each specimen. (1) tip of the snout defined by middle point between the first two frontal incisors, 2) posterior tip of 3rd incisor, 3) anterior tip of canine, 4) posterior tip of canine, (5) anterior tip of the third premolar, (6, 7, 8, 9, 10) outline of carnassial tooth, (11, 12) cusps of molar, (13) anterior tip of molar, (14) posterior tip of molar, (15) junction of the stiff and hard palate. The distance between 3 and 4 describe canine length. The distance between 8 and 10 describe carnassial tooth length. The distance between 1 and 15 describes snout length. Deviation of the specimens analysed from the consensus configuration of landmarks are shown below the skull. Scale bar equals 1cm.
157x100mm (300 x 300 DPI)

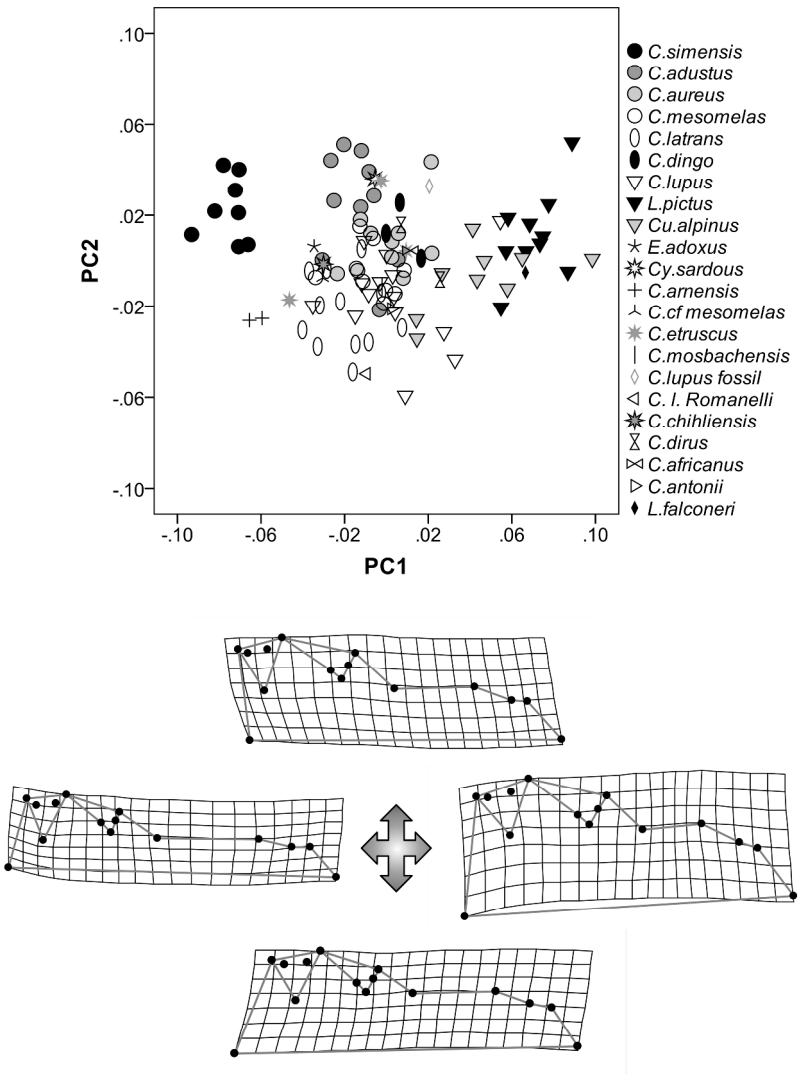

Figure 2 Plot of the first and second principal components. Thin-plate spline diagrams illustrate patterns of landmark displacements along each warp. (Triangles indicate canids in the large dietary category, ellipsoid indicate canids in the medium dietary category and circles indicate canids in the small dietary category. Crosses and stars indicate fossil specimens with an unknown diet category). Below deformation grids from positive to negative RW scores.
259x350mm (300 x 300 DPI)

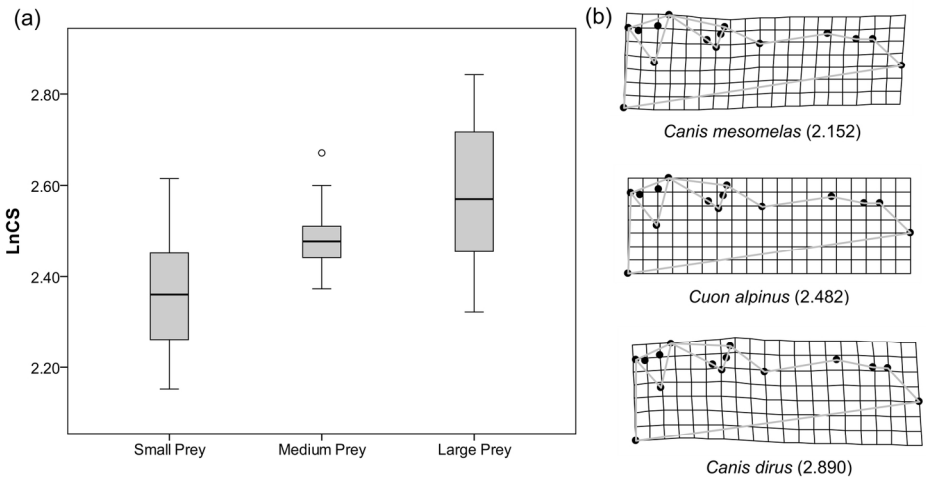

Figure 3 (a) Box plot showing differences in natural log transformed centroid size between diet categories of extant specimens of canid skull (the outlier in the "Medium Prey" category is a specimen of C. latrans); (b) skull shape deformation related to size from the smallest (C. mesomelas) to the largest (C. dirus) canid species. Values in parentheses are ln centroid size.
159x88mm (300 x 300 DPI)

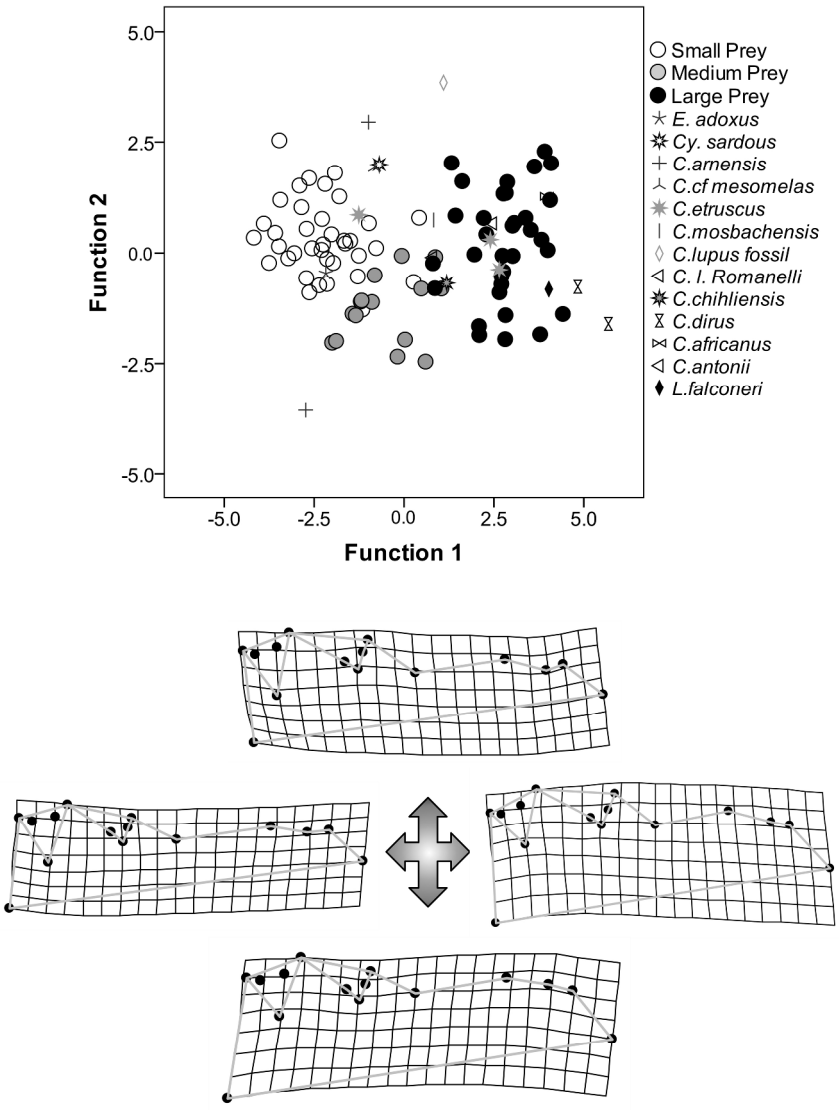

Figure 4 Plot of the first two discriminant functions (DF) extracted from a combination of shape and size variables. Extant specimens are labelled according to their diet categorisation. Fossil specimens are labelled individually. Below deformation grids from positive to negative DF scores.
249x321mm (300 x 300 DPI)

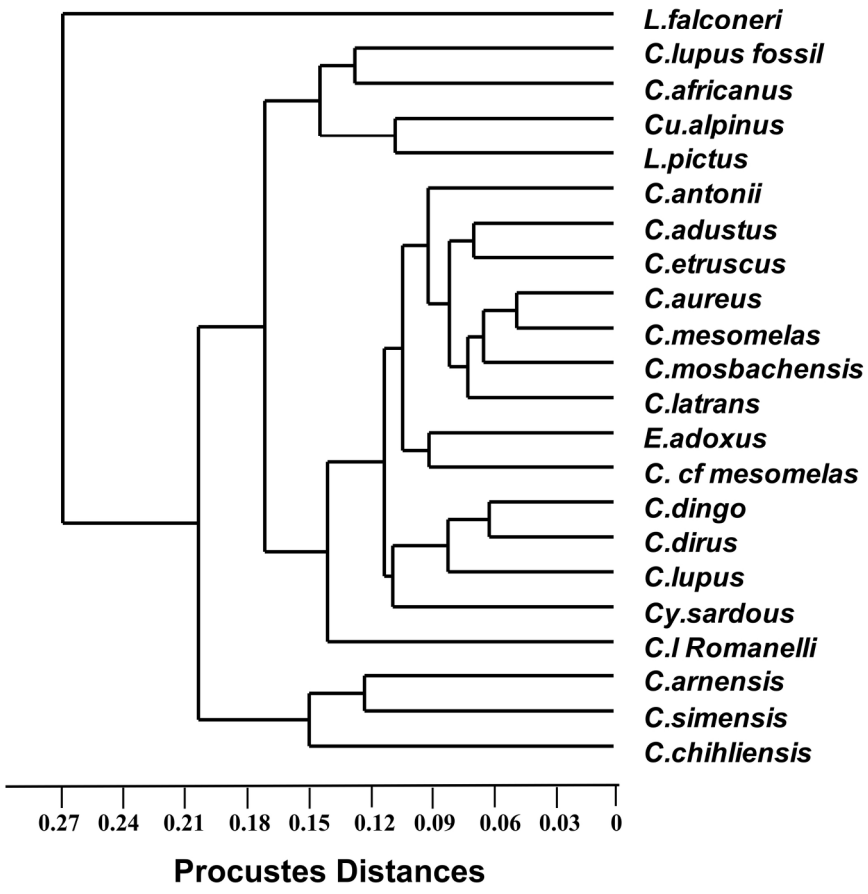

Figure 5 UPGMA Cluster analysis obtained on procustes distances of averaged sample for 23 canid species.
189x202mm (300 x 300 DPI)

TABLE 1

Species	Status	# Specimens	Diet
*Canis lupus**	Extant	14	Large
Canis dingo	Extant	3	Medium
Canis latrans	Extant	12	Medium
Canis aureus	Extant	10	Small
Canis adustus	Extant	10	Small
Canis mesomelas	Extant	9	Small
Canis simensis	Extant	8	Small
*Cuon alpinus***	Extant	9	Large
Lycaon pictus	Extant	10	Large
Eucyon adoxus	Fossil	1	
Cynotherium sardous	Fossil	1	
Canis africanus	Fossil	1	
Canis antonii	Fossil	1	
Canis arnensis	Fossil	2	
Canis chiliensis	Fossil	1	
Canis dirus	Fossil	2	
Canis etruscus	Fossil	3	
Canis cf. *mesomelas*	Fossil	1	
Canis mosbachensis	Fossil	1	
Canis lupus (Grotta Romanelli)	Fossil	1	
Canis lupus (Spain)	Fossil	1	

Lycaon falconeri	Fossil	1

TABLE 2

	Most likely group	P(D | G)	P (G | D)	Second most likely group
Eucyon adoxus	Small	0.726	0.796	Medium
Canis africanus	Large	0.280	1.000	Medium
Canis antonii	Large	0.852	0.998	Medium
Canis arnensis IGF 601V	Small	0.015	0.991	Medium
Canis arnensis IGF 867	Medium	0.006	0.935	Small
Canis chiliensis	Medium	0.192	0.503	Large
Canis dirus cast M11960	Large	0.003	1.000	Medium
Canis dirus cast unknown	Large	0.078	1.000	Medium
Canis etruscus cast MNCN an5006	Small	0.522	0.867	Medium
Canis etruscus SBAU337628	Large	0.839	0.995	Medium
Canis etruscus SBAU398989	Large	0.922	0.996	Medium
Canis. cf. *mesomelas*	Small	0.101	0.941	Medium
Canis mosbachensis	Large	0.126	0.677	Medium
*Canis lupus (*Romanelli*)*	Medium	0.208	0.599	Large
Canis lupus (Spain)	Large	0.000	0.975	Small
Cynotherium sardous	Small	0.073	0.932	Medium
Lycaon falconeri	Large	0.276	1.000	Medium

Appendix 1

List of extant and fossil skull specimens of Canidae.

RMS = Royal Museum of Scotland, Edinburgh UK

NHM = Natural History Museum, London UK

MNCN = Museo Nacional de Ciencias Naturales, Madrid Spain

RMCA = Royal Museum of Central Africa, Tervuren Belgium

ZMF = Zoological Museum Florence University / CE = Museo Doeria, Genoa Italy

Species	Catalogue	Locality	Museum	Period
Canis adustus	66.26	Sakala Ethiopia	NHM, London	Extant
Canis adustus	70.23.27	Kukawa Borno Niger	NHM, London	Extant
Canis adustus	35.9.1.292	Grootefontein	NHM, London	Extant
Canis adustus	70.661	Ethiopia	NHM, London	Extant
Canis adustus	23.1.4.1	Angola	NHM, London	Extant
Canis adustus	26.6.11	Nyasaland	NHM, London	Extant
Canis adustus	RMCA 3921	Zaire	RMCA, Tervuren	Extant
Canis adustus	RMCA 9329	Rwanda	RMCA, Tervuren	Extant
Canis adustus	RMCA 9330	Rwanda	RMCA, Tervuren	Extant
Canis adustus	RMCA 17190	Rwanda	RMCA, Tervuren	Extant
Canis aureus	an 5007	Unknown	Glasgow	Extant
Canis aureus	1937.2.24.49	Dangila Abyssinia	NHM, London	Extant
Canis aureus	23.3.26.14	Laketsana Abyssinia	NHM, London	Extant
Canis aureus	64.21.81	Pircolo Abbai Ethiopia	NHM, London	Extant
Canis aureus	70.66	Ethiopia 2500m	NHM, London	Extant
Canis aureus	36.5.20.6	Goulse Bale Abyssinia	NHM, London	Extant
Canis aureus	36.5.20.4	Arussi Abyssinia	NHM, London	Extant
Canis aureus	75.2312	Assam	NHM, London	Extant
Canis aureus	67.69	Sri Lanka	NHM, London	Extant
Canis aureus	1892.7.16.1	Luxor, Egypt	NHM, London	Extant
Canis dingo	an5007	Unknown	Glasgow	Extant
Canis dingo	140c	Unknown	Glasgow	Extant
Canis dingo	1952.4.1.2	Australia	NHM, London	Extant
Canis latrans	2003.130.02	Unknown	RMS, Edinburgh	Extant
Canis latrans	2003.130.03	Unknown	RMS, Edinburgh	Extant
Canis latrans	2003.130.64	Unknown	RMS, Edinburgh	Extant

Species	Catalogue	Locality	Museum	Period
Canis latrans	2003.130.05	Unknown	RMS, Edinburgh	Extant
Canis latrans	2003.130.07	Unknown	RMS, Edinburgh	Extant
Canis latrans	2003.130.08	Unknown	RMS, Edinburgh	Extant
Canis latrans	2.3.7.4	Penington British Columbia	NHM, London	Extant
Canis latrans	94.5.9.4	Chapham New Mexico	NHM, London	Extant
Canis latrans	98.12.21.1	Chihout Mt. British Columbia	NHM, London	Extant
Canis latrans	40.82.1	San Quintin Lower California Mexico	NHM, London	Extant
Canis latrans	2.82.2	Jouchood Hillo Asauriboia New Mexico	NHM, London	Extant
Canis latrans	10909	Hansoon Lagoon L.C. Mexico	NHM, London	Extant
Canis lupus	an4560	Unknown	Glasgow	Extant
Canis lupus pambasilens	19.7.15.4	McMillan River Youkon Territories	NHM, London	Extant
Canis lupus gigas	63.2.24.51	Fort Langley New Wesminster British Columbia	NHM, London	Extant
Canis lupus gigas	63.2.24.31	British Columbia	NHM, London	Extant
Canis lupus pambasilens	19.7.15.5	McMillan River Youkon Territories	NHM, London	Extant
Canis lupus	1852.3.24.4_ 168.c.	Azraq, Jordan	NHM, London	Extant
Canis lupus arabs	84.1312	Unknown	NHM, London	Extant
Canis lupus arctos	86.1595	Ellesmere island, Canada	NHM, London	Extant
Canis lupus occidentalis	1855.5.14.11	"Arctic" America, Canada	NHM, London	Extant
Canis lupus pallipes	1863.12.28.1 4	India	NHM, London	Extant
Canis lupus chanco	1875.4.10.1_ 1670.a.	Near Tshommeriri lake, Tibet	NHM, London	Extant
Canis lupus	1935.8.5.1	Bosnia, Yugoslavia	NHM, London	Extant
Canis lupus	1937.2.10.2	Abrantos, S. of Taqus, Portugal	NHM, London	Extant

Species	Catalogue	Locality	Museum	Period
Canis lupus chanco	1961.9.21.2	Khumbu, East Nepal	NHM, London	Extant
Canis mesomelas	24.1.1.91	Samumba Singida	NHM, London	Extant
Canis mesomelas	29.8.14.2	Somaliland	NHM, London	Extant
Canis mesomelas	23.3.4.23	Mlawa Mkalam	NHM, London	Extant
Canis mesomelas	69.10.24.7	Anseba	NHM, London	Extant
Canis mesomelas	25.1.2.210	Unknown	NHM, London	Extant
Canis mesomelas	28.9.11.138	Unknown	NHM, London	Extant
Canis mesomelas	1991.586	Zimbawe	NHM, London	Extant
Canis mesomelas	RMCA 2145	Ziwani, Brit East A	RMCA, Tervuren	Extant
Canis mesomelas	RMCA 2164	Ziwani, Brit East A	RMCA, Tervuren	Extant
Canis simensis	23.10.10.1	Arusi 1300 m	NHM, London	Extant
Canis simensis	24.8.7.11	Chilalo Arussi Galla	NHM, London	Extant
Canis simensis	36.5.20.4	Chilalo W.Arussi Abyssinia	NHM, London	Extant
Canis simensis	24.8.9.10	Gojam Abyssinia	NHM, London	Extant
Canis simensis	24.8.7.12	Simien	NHM, London	Extant
Canis simensis	2.4.00	Abyssinia	NHM, London	Extant
Canis simensis	ZMF 13718	Senneti Platue	ZMF, Florence	Extant
Canis simensis	CE 818	Arussi Abyssinia	Museum Doria, Genoa	Extant
Cuon alpinus	34.10.4.4	Ramnagar Kumaon	NHM, London	Extant
Cuon alpinus dukhnensis	No catalogue	Unknown	RMS, Edinburgh	Extant
Cuon alpinus javanicus	35.3.22.1	Chamrajnagar S.Mysore	NHM, London	Extant
Cuon alpinus javanicus	1939.1.10.24	Masangaudi Bilgiris S.India	NHM, London	Extant
Cuon alpinus javanicus	1937.12.3.31	Shan States Upper Bhurma	NHM, London	Extant
Cuon alpinus javanicus	34.9.18.2	Tian Shan (Central Asia)	NHM, London	Extant
Cuon alpinus javanicus	5.11.19.1	Ussuri River Manchuria	NHM, London	Extant

Species	Catalogue	Locality	Museum	Period
Cuon alpinus javanicus	88.2.5.22_159.d.	Anamalai Hills, Coimbatore, S.India	NHM, London	Extant
Cuon alpinus dukhnensis	1936.4.8.1	India	NHM, London	Extant
Lycaon pictus	61.976	Kabompo Dist. (Rhodesia)	NHM, London	Extant
Lycaon pictus	10.10.3.2	Linyanti R.N.Banr. Rhodesia	NHM, London	Extant
Lycaon pictus	1.4.26.3	Rift Valley	NHM, London	Extant
Lycaon pictus	49.122	Mont Kenya	NHM, London	Extant
Lycaon pictus	Z1908 077c	Unknown	RMS, Edinburgh	Extant
Lycaon pictus	1963.9.30.1	(P) Zool. Soc. London, Africa	NHM, London	Extant
Lycaon pictus	1969	(P) Zool. Soc. London, Africa	NHM, London	Extant
Lycaon pictus	RCMA 15896	buta, Zaire	RMCA, Tervuren	Extant
Lycaon pictus	RCMA 1096	buta, Zaire	RMCA, Tervuren	Extant
Lycaon pictus	RCMA 2144	camp simba ziwani, Brit East A	RMCA, Tervuren	Extant
Cynotherium sardous	CB 848022	Corbeddu, Sardinia	In: Lyras et al. (2006) JVP 26:735-745	Pleistocene
Canis dirus	M11960	Cast from Rancho La Brea	NHM, London	Late Pleistocene
Canis dirus	unknown	Cast from Rancho La Brea	NHM, London	Late Pleistocene
Canis lupus (fossil)	P3580	Grotta Romanelli, Puglia	Pigorini, Rome	Middle Pleistocene
Canis lupus (fossil)	MNCN 31649A	Unknown	MNCN, Madrid	Upper Pleistocene
Canis mosbachensis	Unknown	Untermmassfield	from: Sotnikova (1998)	Middle Pleistocene
Canis chihliensis	IVPP V 18333.1	Nihewan	From Tong et al., (2012)	Pleistocene, ca. 1.3 Ma - 1.8 Ma
Eucyon adoxus	RSS45	Perpignan, France	cast_MNCN Madrid	Pliocene
Canis antonii	Cast of F:AM 97052	Nihewanian, Shanxi Province, China	Florence	Pliocene (3.5 Ma)
Canis cf. mesomelas	KNM-ER3667	Koobi Fora, East Africa	Kenya National Museum	Plio-Pleistocene

Species	Catalogue	Locality	Museum	Period
Canis africanus	OLD74	Olduvai Bed I	Kenya National Museum	Plio-Pleistocene (c.ca 1.9 Ma)
Canis arnensis	IGF 601V	Valdarno (Italy)	Florence	Plio-Pleistocene (c.ca 1.9 Ma)
Canis arnensis	IGF867	Valdarno (Italy)	Florence	Plio-Pleistocene (c.ca 1.9 Ma)
Canis etruscus	an5006c	Olivola	cast_MNCN Madrid	Plio-Pleistocene (c.ca 1.9 Ma)
Canis etruscus	SBAU337628	Pantalla, Italy	from Cherin et al. (2014)	Plio-Pleistocene (c.ca 1.9 Ma)
Canis etruscus	SBAU398989	Pantalla, Italy	from Cherin et al. (2014)	Plio-Pleistocene (c.ca 1.9 Ma)
Lycaon falconeri	IGF 865	Valdarno (Italy)	Florence	Plio-Pleistocene (c.ca 1.9 Ma)